

# Photostability of thiol-capped CdTe quantum dots in living cells: the effect of photo-oxidation

J Ma<sup>1,2</sup>, Ji-Yao Chen<sup>1,3,5</sup>, J Guo<sup>4</sup>, C C Wang<sup>4</sup>, W L Yang<sup>4</sup>, L Xu<sup>3</sup>  
and P N Wang<sup>3</sup>

<sup>1</sup> Department of Physics, Fudan University, Shanghai 200433, People's Republic of China

<sup>2</sup> State Key Laboratory of Applied Surface Physics, Fudan University, Shanghai, People's Republic of China

<sup>3</sup> State Key Lab for Advanced Photonic Materials and Devices, Fudan University, Shanghai, People's Republic of China

<sup>4</sup> Department of Macromolecular Science and Key Laboratory of Molecular Engineering of Polymers, Fudan University, Shanghai, People's Republic of China

E-mail: [jychen@fudan.edu.cn](mailto:jychen@fudan.edu.cn)

Received 10 September 2005, in final form 10 February 2006

Published 28 March 2006

Online at [stacks.iop.org/Nano/17/2083](http://stacks.iop.org/Nano/17/2083)

## Abstract

The photostability of thiol-capped CdTe quantum dots (QDs) in *Euglena gracilis* (EG 277) and human embryonic kidney (HEK 293) cells was studied. The photobleaching for the cellular QDs is dependent both on the irradiation power density and the QD local concentration. The photostability of cellular QDs is better than that of chlorophyll in EG 277 cells and of green fluorescence protein (GFP) in HEK 293 cells, and is much better than that of FITC when the local concentration of QDs is not too low. The photobleaching of cellular QDs was remarkably reduced in the nitrogen treated EG 277 cells, indicating that photobleaching in living cells mainly results from photo-oxidation. The effect of photo-oxidation on QD photobleaching was further confirmed by comparing the situations in oxygen treated and nitrogen treated QD aqueous solutions. The photobleaching rate is related to the irradiation power density and the local density of QDs. The higher irradiation power density and oxygen abundance and lower QD concentration will result in a higher photobleaching rate.

(Some figures in this article are in colour only in the electronic version)

 Supplementary data files are available from [stacks.iop.org/Nano/17/2083](http://stacks.iop.org/Nano/17/2083)

## 1. Introduction

The technique of fluorescence probes opened a new way to visualize cellular structure and study cellular processes [1, 2]. The commonly used fluorescence probes are organic fluorophores such as rhodamine and fluorescein isothiocyanate (FITC). However, these organic dyes have limitations due to their low photostability, narrow absorption bands and broad emission spectra [3]. Along with the development of the hydrophilic photo-luminescent

semiconductor quantum dots (QDs) [3, 4], cellular labelling with these nanosized QDs has great potential applications in cellular imaging [5–7]. These QDs are believed to have advantages as compared with the conventional organic probes, since they have higher photoluminescence quantum efficiency and their luminescence peaks are tunable with their sizes [8–10]. Moreover, the absorption spectrum of the QDs is a wide continuum from the bandgap to the ultraviolet so that the excitation of these QDs is flexible [11]. However, when used as luminescent labels in cells, the QDs must be rendered hydrophilic to dissolve in aqueous buffers. Usually,

<sup>5</sup> Author to whom any correspondence should be addressed.

the synthesis of QDs, such as CdSe and CdS, is carried out in organic solvents at high temperature to form the cores of QDs, and then these cores are capped with a thin layer of a higher bandgap material such as ZnS or CdS to passivate the surface and increase the fluorescence efficiency. The hydrophobic surface of these QDs with a core-shell structure should be treated again with a ligand such as mercaptoacetic acid to become hydrophilic [12]. In an alternative way, the QDs can also be synthesized directly in aqueous solution to have a hydrophilic surface, such as the thiol-stabilized CdTe QDs [13]. These water-soluble QDs can meet the basic requirement in biomedical applications.

A typical feature of the QDs is their photostability, which is especially important in cellular labelling. Although the photostability of water-soluble QDs was reported to be much better than rhodamine and FITC [3, 4, 14], the photochemical instability of the thiol-coated QDs was also reported and the mechanism is not yet clear [15, 16]. In the present work, the photostability of thiol-capped CdTe QDs in two kinds of living cells was studied, and compared with that of FITC, GFP and native chlorophyll. We found that the photostability of the cellular QDs was dependent on their local concentration and it became worse when the QD concentration was very low. The photobleaching mechanism of the cellular QDs was shown to be the oxygen dependent photo-oxidation.

## 2. Experimental details

### 2.1. Synthesis of CdTe QDs

The thiol-capped CdTe QDs were fabricated in our laboratory by the hydrothermal route, which is believed to be a simple and efficient method [17]. The details of the procedure could be found in our previous work [18]. Briefly, with a molar ratio of 2:1, sodium borohydride was used to react with tellurium in water to prepare sodium hydrogen telluride (NaHTe). Fresh solutions of NaHTe were then diluted by N<sub>2</sub>-saturated deionized water to 0.0467 M for further use. CdCl<sub>2</sub> (1 mmol) and mercaptoacetic acid (1.2 mmol) were dissolved in 50 ml of deionized water. Stepwise addition of NaOH solution adjusted the precursor solution to pH = 9. Then, 0.096 ml of oxygen-free solution containing fresh NaHTe, cooled to 0 °C, was added to 10 ml of the above prepared precursor solution and stirred vigorously. Finally, the solution, with a faint yellow colour, was put into a Teflon-lined stainless steel autoclave with a volume of 15 ml. The autoclave was maintained at the reaction temperature (200 °C) for a certain time and then cooled to the room temperature by a hydro-cooling process. The as-prepared CdTe QDs, dispersed in water, were precipitated from solution using excess ethanol. Then, these solutions were centrifuged to harvest QDs in the bottom of the centrifuging tube. The obtained QD powders were dried in vacuum and brought into a nitrogen-atmosphere box for subsequent use. A stock solution of QDs (1 mg ml<sup>-1</sup>) was made for experiments by resolving a certain amount of QD powder into a corresponding volume of water. The luminescence of the obtained QD solution was centred at 605 nm with a luminescent quantum yield of 0.4 [18].

### 2.2. Cell culture

**2.2.1. *Euglena gracilis*.** *Euglena gracilis* 277 (EG 277) was procured from the Institute of Hydrobiology, Chinese Academy of Sciences (Wuhan). The details of the cell culture can be found in the literature [19]. In normal culture conditions, the cells were cultured in a 250 ml flask containing 100 ml liquid culture medium. The cell flask was exposed in 12 h irradiation (2300 lx)/12 h dark cycles at 25 °C for 48–72 h. To prepare the cell samples, the cells were centrifuged three times in deionized water to remove the culture medium. The washed cells were then re-suspended in water, and incubated with QDs (0.1–0.3 mg ml<sup>-1</sup>) for one day. After incubation, the cell samples were further washed by three cycles of centrifugation to remove the unbound QDs in the solution. The QD treated cells were suspended in water again with a cell density of 10<sup>6</sup> ml<sup>-1</sup>, and were ready for measurement. The tolerance of EG 277 cells to QDs is very strong. Even when incubated with QDs at a concentration of 0.5 mg ml<sup>-1</sup>, no detectable damage to cells was found.

**2.2.2. HEK 293 cells.** The HEK 293 cells, originally derived from a human embryonic kidney, were purchased from the cell bank of Shanghai Science Academy [20]. The cells were cultured in DEME medium containing 10% foetal calf serum, 100 units ml<sup>-1</sup> penicillin, 100 µg ml<sup>-1</sup> streptomycin, and 100 µg ml<sup>-1</sup> neomycin in a fully humidified incubator at 37 °C with 5% of CO<sub>2</sub>. The cells were subcultured in tissue culture flasks to keep them in an exponential growth phase for use in experiments.

To stain the cells with QDs, the cells in culture flasks were incubated with QDs (0.15 mg ml<sup>-1</sup>) in DMEM medium for 4 h in an incubator. Then, these QD loaded cells were washed with PBS for three times and fixed with 10% formol (pH = 7.4) for 10 min at room temperature. After washing again, these cell samples were ready for the fluorescence experiments. The HEK 293 cells are fragile to the QDs of high incubation concentration (over 0.5 mg ml<sup>-1</sup>). Under incubation conditions in this experiment, the cells were in the normal state.

For GFP labelling in 293 cells, the EGFP-C1 (Clontech), an expression vector containing an enhanced green fluorescent protein coding region, was transfected into HEK 293 cells using liposomal transfection reagent in accordance with the standard protocol [21]. Transfection was carried out in a 35 mm culture dish by adding 1 µg of plasmid DNA and 3 µg of Fugene 6 liposomal transfection reagent (Boehringer) according to the manufacturer's instructions. The transfected cells were checked by a fluorescence microscope.

FITC labelling of cells was conducted with immunostaining. The HEK 293 cells adhered on slide glass were incubated with phalloidin-FITC for 30 min, and then washed and mounted with a drop of 50% glycerol.

### 2.3. Experimental measurements

**2.3.1. Cellular imaging.** The cellular images were acquired with a confocal laser scanning microscope (Olympus, FV-300, IX71). The intracellular distributions of QDs, FITC and GFP could be obtained at the same time by recording their luminescence or fluorescence signals in different channels

using a set of filters. A water immersion objective (60 $\times$ ) and a matched pinhole were used in the measurements. Using the  $z$ -scan mode, the images in different layers could be recorded to obtain the three-dimensional distributions in the cells. From these images, the intracellular distributions of QDs and the relative luminescence intensities were obtained.

**2.3.2. Photobleaching measurement.** The photobleaching of the cellular QDs and other cellular fluorophores were measured with the point-stay mode of the microscope. In this mode, the focused laser beam was fixed at the selected spot of the sample and the time-dependent luminescence/fluorescence intensities were recorded by a photomultiplier tube (PMT) with the appropriate filter sets. The spot size of the laser beam focused by a 60 $\times$  objective lens was about 1  $\mu\text{m}$  in diameter. The laser power on the sample was measured with a laser-power meter (Coherent), and the irradiation power density could be calculated.

The photobleaching of QDs in aqueous solution was performed in a small cuvette under a continuous laser irradiation at 532 nm (Coherent, Nd:YVO<sub>4</sub>). The decay of the photoluminescence (PL) signal from QDs was measured with a PMT and a band-pass filter (585–640 nm) and recorded by a digital oscilloscope.

The photo-oxidation effect on photobleaching of cellular QDs in EG 277 was investigated by the confocal microscope. A suspension of QD loaded cells in a test-tube was bubbled with nitrogen gas for 1 h. The suspension was then sealed between a piece of slide glass and a piece of cover slip for the microscopic measurements. All the procedures were carried out in a glove box with nitrogen atmosphere. Meanwhile, the photobleaching of QD loaded cells without N<sub>2</sub> treatment was also measured under the same conditions as a comparison.

**2.3.3. Average concentration of cellular QDs.** To estimate the amount of cellular QDs, the alkali extraction method was used. After incubation with QDs, the HEK 293 cells were washed three times to remove unbound QDs and then digested. The cell density in each sample suspension was counted in the microscope with the cell-counter. These cell samples were then incubated in NaOH solution (0.1 M) for 2 h to thoroughly destroy the whole cells as well as the cellular organelles and extract the cellular QDs into the solutions. These sample solutions were centrifuged, and the QD containing supernatant in each sample was collected, respectively. The PL spectra and the intensities at the spectral peak of these supernatants were measured by a fluorescence spectrophotometer (Hitachi, F-2500) using the excitation wavelength of 400 nm. Meanwhile, a calibration curve of the peak intensity as a function of QD concentration was made as shown in the supporting information. Comparing the PL intensities of the supernatants with the calibration curve, the average amount of cellular QDs per cell can be calculated according to the cell density counted.

A similar procedure was carried out for EG 277 to estimate the QD concentration.

### 3. Results and discussion

In EG 277 cells, the chlorophyll (mainly chlorophyll a- and chlorophyll ab-proteins [22]) is the native fluorophore, which

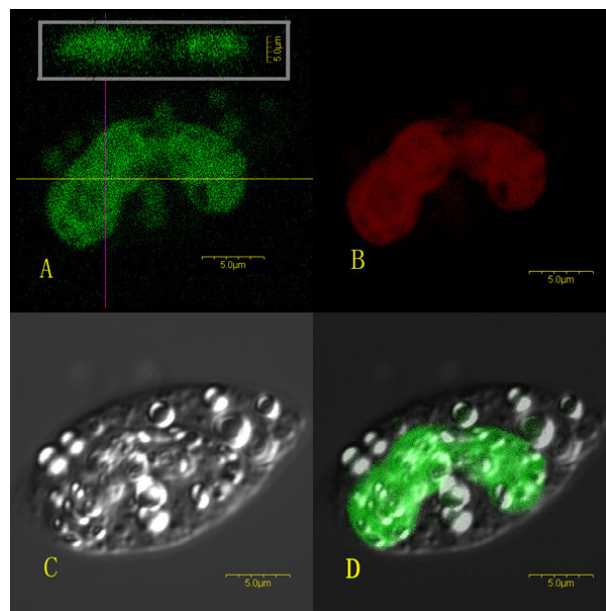


**Figure 1.** Micrographs of an EG 277 cell. (A) PL images of cellular QDs in  $x$ - $y$  (main one) and  $x$ - $z$  (upper one) planes. (B) Fluorescence image of chlorophyll; (C) the DIC image. (D) The merged image of (A) and (C).

emits fluorescence peaked around 685 nm, while the observed PL of cellular QDs in EG 277 is peaked around 605 nm. When the cells were excited with a 488 nm laser beam in a confocal microscope, the fluorescence images of cellular QDs and chlorophyll were recorded simultaneously in channel 1 with a 585–630 nm band-pass filter and in channel 2 with a 630 nm long-pass filter, respectively. Figure 1 shows the images obtained in the two channels as well as the differential interference contrast (DIC) image acquired simultaneously in a transmission channel to exhibit the cell morphology. The cells have been incubated with 0.2 mg ml<sup>-1</sup> QDs for one day. Figure 1(A) demonstrates the intracellular distribution of QDs in an EG 277 cell, where the main image shows the cellular QDs in the  $x$ - $y$  plane and the upper profile exhibits the QD distributions in the  $x$ - $z$  plane along the marked line in the main image obtained by  $z$ -scanning. The QDs were found to distribute diffusely inside the cell, but no QDs were detected in the outer membrane of the cell. After alkali extraction, the average amount of QDs per cell was measured to be about  $8.75 \times 10^{-7} \mu\text{g}$  or  $2.3 \times 10^6$  QDs (see supporting information available at [stacks.iop.org/Nano/17/2083](https://stacks.iop.org/Nano/17/2083)). The volume of a single EG 277 cell can be estimated to be 470  $\mu\text{m}^3$ . The average concentration of cellular QDs in EG 277 cells was calculated to be 1.86 mg ml<sup>-1</sup>, which is much higher than the incubation concentration of QDs (0.2 mg ml<sup>-1</sup>), indicating that the cells actively engulfed QDs during the incubation. This phenomenon is not so surprising since the EG cells tend to internalize the outside materials as reported previously [23].

Based on the images shown in figure 1, we can select some parts in the cell to study photobleaching. The typical photobleaching curves of the chlorophyll and QDs in an EG277 cell, under an excitation power density of  $8 \times 10^{-4} \text{ W } \mu\text{m}^{-2}$ , are shown in figure 2. Both the cellular QDs and chlorophyll

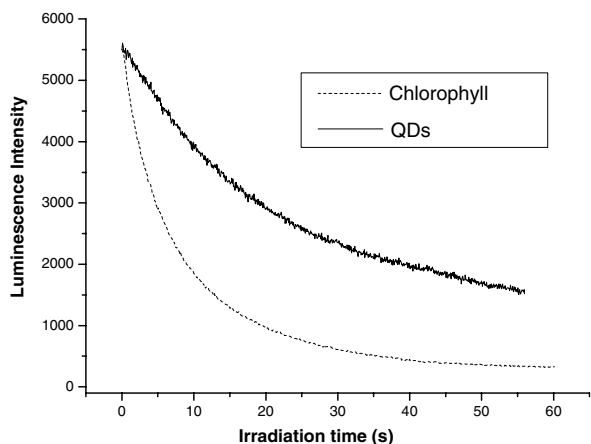


**Figure 2.** Photobleaching of QDs and chlorophyll in an EG 277 cell as a function of irradiation time.

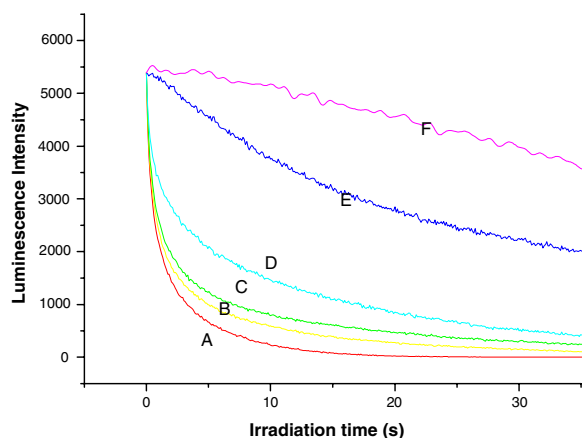


**Figure 3.** The photobleaching of cellular QDs in an EG 277 cell as a function of time. The irradiation power densities (488 nm) are  $6.4 \times 10^{-3}$  (A),  $4.8 \times 10^{-3}$  (B),  $3.2 \times 10^{-3}$  (C),  $1.6 \times 10^{-3}$  (D),  $8 \times 10^{-4}$  (E) and  $8 \times 10^{-5}$  (F)  $W \mu m^{-2}$ .

were photobleached as a function of irradiation time but the QDs seem more stable than the native chlorophyll.

The dependence of QD photobleaching in the EG 277 cells on the irradiation power density was shown in figure 3. As can be seen, under a low power density of  $8 \times 10^{-5} W \mu m^{-2}$ , the QDs were very stable. When the power density was increased to  $6.4 \times 10^{-3} W \mu m^{-2}$ , the QDs were bleached in a few seconds, indicating that the irradiation power density plays an important role in photobleaching. Thus, for the imaging measurements, over-irradiation should be avoided.

The various cellular concentrations (relative) of QDs in different cell groups were obtained by incubating the EG 277 cells with different QD concentrations, respectively, and then measuring the relative PL intensities for each cell group. Table 1 shows that the cellular QD concentration increased with the QD incubation concentration, but tended to saturate in a concentration over  $0.2 mg ml^{-1}$ . The photobleaching curves with different QD cellular concentrations are shown in figure 4, demonstrating that the photobleaching is slower when the cellular QD concentration is higher. The photobleaching times (when PL intensity decreased to half) are also listed in table 1,

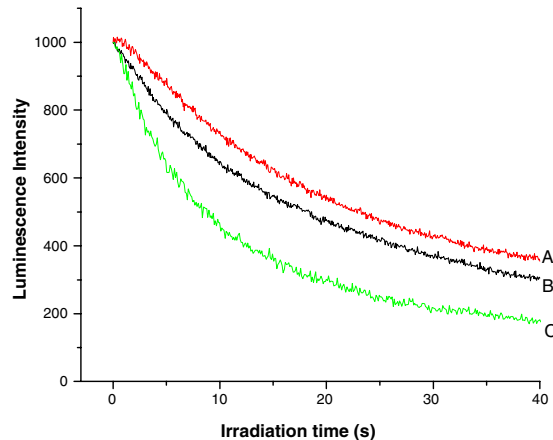


**Figure 4.** The photobleaching of cellular QDs in EG 277 cells as a function of irradiation time for different QD incubation concentrations (curves have been normalized). (A)  $0.3 mg ml^{-1}$ ; (B)  $0.2 mg ml^{-1}$ ; (C)  $0.1 mg ml^{-1}$ . The irradiation power density is  $8 \times 10^{-4} W \mu m^{-2}$ .

**Table 1.** The photobleaching time (the time for PL intensity decreased to half) of QDs in EG 277 cells with different QD incubation concentrations. For each group, 10–20 cells were measured and the data were calculated statistically. The irradiation power density is  $8 \times 10^{-4} W \mu m^{-2}$ .

Incubation concentration of QDs ( $mg ml^{-1}$ )	Concentration of cellular QDs (relative)	Bleaching time (s)
0.3	$1000 \pm 99$	$32.1 \pm 9.4$
0.2	$834 \pm 203$	$24.0 \pm 7.7$
0.1	$402 \pm 75$	$7.1 \pm 1.6$

demonstrating further that the average bleaching time in cells with higher cellular concentration is significantly longer than that of the cells with the lower cellular concentration ( $24.0 \pm 7.7$  to  $7.1 \pm 1.6$  s). These results indicate that the photobleaching of the cellular QDs is cellular concentration dependent.

The intracellular distribution of QDs in HEK 293 cells depicted in figure 5 shows that the cellular uptake of QDs also occurred in HEK 293 cells. Compared with EG 277 cells (figure 5(b)), the distribution patterns are different. The QDs are more uniformly distributed in the EG 277 cells, but are patchy in appearance in the cytoplasm of HEK 293 cells, which might be due to their different cellular structures. Figure 5(d) shows the QD distribution in  $x-y$  and  $x-z$  planes in an HEK 293 cell, demonstrating that the QDs are not only bound to the plasma membrane but also localized in the cytoplasm of the cell. The local brightness in the images is proportional to the local concentration of QDs. Under the same measuring conditions, the luminescence brightness in HEK 293 cells (figure 5(a)) is much lower than that in EG 277 cells (figure 5(b)), corresponding to a lower local concentration of QDs in HEK 293 cells. With alkali extraction (see supporting information available at [stacks.iop.org/Nano/17/2083](http://stacks.iop.org/Nano/17/2083)), the average amount of QDs per HEK 293 cell was determined to be about  $2.32 \times 10^{-7} \mu g$  (namely  $6.1 \times 10^5$  QDs per cell), which is much lower than that in EG 277 cells, but is comparable to that in Chinese hamster ovary cells [24]. The average

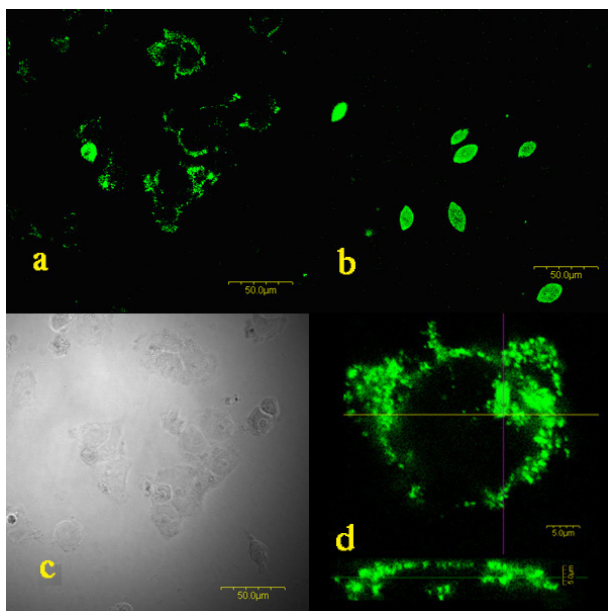


**Figure 5.** PL images of cellular QDs. (a) HEK 293 cells; (b) EG 277 cells; (c) DIC image of the HEK 293 cells in (a); (d) luminescence images in  $x$ - $y$  (main one) and  $x$ - $z$  (bottom one) planes from the cellular QDs in an HEK 293 cell. Excitation, 488 nm; filter, 585–630 nm.

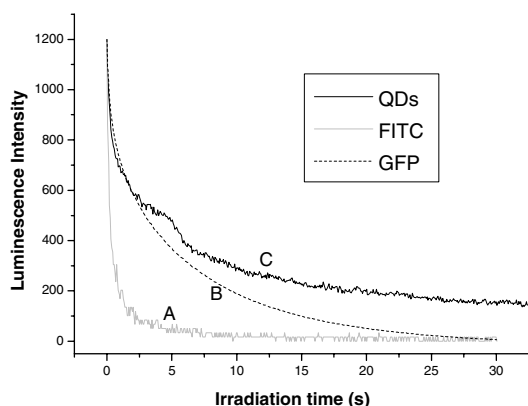


**Figure 6.** The photobleaching curves of (A) FITC, (B) GFP and (C) QDs in HEK 293 cells. The irradiation power density was  $8 \times 10^{-4} \text{ W } \mu\text{m}^{-2}$ , the same as that in figure 2.

volume of a single HEK 293 cell is about  $1200 \mu\text{m}^3$ , which is larger than that of an EG 277 cell, as shown in figure 5. The average intracellular concentration of QDs in HEK 293 cells can be estimated to be  $0.19 \text{ mg ml}^{-1}$ . Compared with the QD incubation concentration of  $0.15 \text{ mg ml}^{-1}$ , the active internalization of QDs by HEK 293 cells may also have occurred. For these mammal cells, endocytosis was suggested as the mechanism of the internalization [25].

The photobleaching in HEK 293 cells was performed under the same irradiation conditions as that for EG 277 cells. The photobleaching curves of cellular QDs, FITC and GFP in HEK 293 cells are shown in figure 6. Although all three species were photobleached, the bleaching of QDs is a little bit slower than that of GFP, and much slower than that of FITC. It should be noted that under the same irradiation power

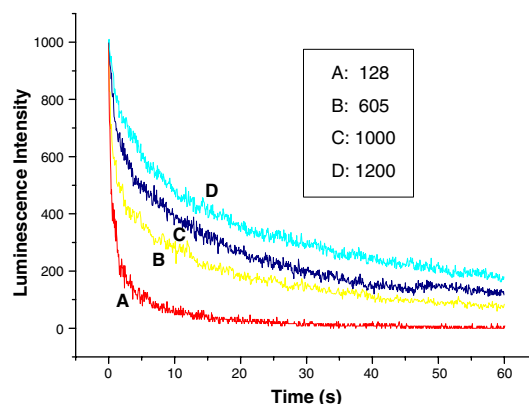


**Figure 7.** Photobleaching curves with different local QD concentrations in an HEK 293 cell. The bleaching curves were measured in the areas with different brightnesses and have been normalized. The values in the inset are the initial luminescent brightnesses of each curve. The power density of the irradiation at 488 nm is  $8 \times 10^{-4} \text{ W } \mu\text{m}^{-2}$ .

density the photobleaching of QDs in HEK293 cells (figure 6) is much faster than that in EG 277 cells (figure 2). The cellular QDs have lost half of their luminescence intensities within 20 s in EG 277 cells, but within only 3 s in HEK 293 cells. What causes such a remarkable difference? The difference of cellular QD concentrations must be one of the reasons. As discussed above, the average concentration as well as the local concentration of QDs in EG277 cells is obviously higher than that in HEK293 cells. Hence, the cellular QD concentration must be an important factor for the photostability of QDs in cells.

As the distribution of QDs in HEK293 cells is not uniform (figure 5(a)), these cells are suitable samples to study the dependence of photobleaching on the local concentration of QDs. The relationship between photobleaching and local concentration was studied by choosing different areas with different brightnesses in the same cell. The results are shown in figure 7, where the bleaching curves were normalized and the value of the initial brightness of each curve at the start point was listed in the inset. These values correspond to the local concentrations of QDs at these irradiated spots. The lower the QD local concentration, the faster the bleaching, indicating that photobleaching is inversely proportional to the QD local concentration. This effect was confirmed by repeating measurements for about 30 cells.

Though QDs are believed to be relatively photostable, our results indicate that the thiol-capped QDs would still be photobleached, especially when the local concentration of cellular QDs is low. Therefore, when these QDs are used as the probes in cellular labelling, reaching a certain cellular concentration level is a critical condition. When the cellular concentration of QDs is too low, their photobleaching is comparable with or even worse than that of FITC. The advantage of their photostability would be lost.

In bio-medical applications, the QDs must be dissolved in aqueous buffers. The thiol-capping is the most popular way to make the QDs water soluble [26]. In this work, the thiol-capping was automatically finished in the synthetic reaction. Whether thiol-capped or thiol-coated, the QDs [14]

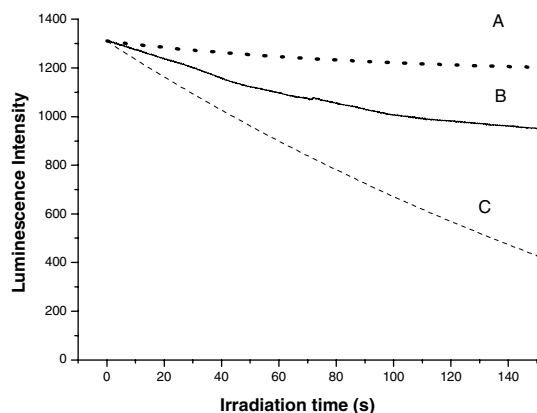


**Figure 8.** Photobleaching curves in aqueous solutions of QDs ( $0.07 \text{ mg ml}^{-1}$ ). The power density of irradiation at  $532 \text{ nm}$  was  $80 \text{ mW mm}^{-2}$ . (A)  $\text{N}_2$  bubbled; (B) in air; (C)  $\text{O}_2$  bubbled.

are photobleachable. Therefore, the concentration effect on photobleaching is probably a common problem of thiol covered QDs. When these QDs are used in cellular imaging, the particular local concentration of QDs should be taken into account for obtaining satisfactory signals.

Why would the thiol-capped QDs be bleached under irradiation? Thiol-related photo-oxidation has been proposed [14]. However, to our knowledge, no experimental evidence has directly demonstrated it so far, though the deduction seems reasonable. Photo-oxidation needs two necessary conditions, light and oxygen. When the oxygen exists in the system, the increase of the light intensity should accelerate the bleaching of QDs. Such an effect is confirmed in this work as shown in figure 3. Nevertheless, the role of oxygen for photobleaching should also be confirmed, which was first studied in QD water solutions. By bubbling the pure oxygen gas in a QD aqueous solution, the  $\text{O}_2$  density in the solution was increased to the maximum. When nitrogen gas was used to perform bubbling, the oxygen molecules were purged out of the solution and the system became nearly oxygen free. The photobleaching effects in QD aqueous solutions were comparatively measured in air, full oxygen and full nitrogen environments, respectively, as shown in figure 8. The oxygen effect on QD photobleaching is clearly demonstrated. When the oxygen was excluded (curve A), the QDs were very photostable. The more oxygen existed, the worse the photostability was (curves B and C). In the air condition, the oxygen density in aqueous solution in air is about  $1.82 \times 10^{17} \text{ molecules ml}^{-1}$ . The QD concentration of  $0.07 \text{ mg ml}^{-1}$  used in the experiment corresponds to  $1.87 \times 10^{14} \text{ QDs ml}^{-1}$ . Thus, each QD is surrounded by almost 1000 oxygen molecules, providing a sufficient environment for the photo-oxidation. In the full oxygen condition, the oxygen density in water is five times higher than that in air, so that the bleaching happened at the highest rate.

The photo-oxidation effect on the bleach of QDs in EG 277 cells was also studied using the same method of nitrogen treatment (see section 2.3.2). Figure 9 demonstrates a comparison of the photobleaching for EG 277 cells,  $\text{N}_2$  treated (curves 1 and 2) and untreated (in air) (curves 3 and 4). The differences between the two situations are obvious, indicating that the photo-oxidation must be the main

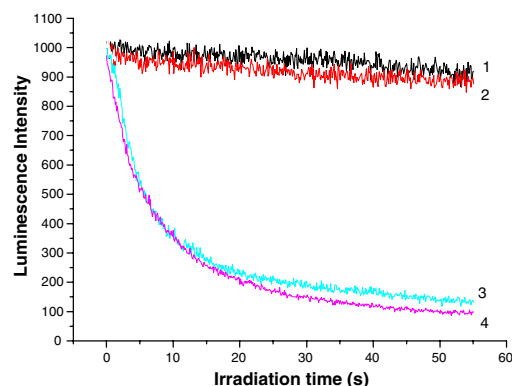


**Figure 9.** Photobleaching of cellular QDs in  $\text{N}_2$  treated (curves 1 and 2) and untreated (curves 3 and 4) EG 277 cells.

reason for the photobleaching of cellular QDs. These results provide unambiguous evidence that photo-oxidation leads to the photobleaching of QDs either in solution or in living cells. Although the local oxygen density varies from place to place in a living cell, it almost keeps constant with time in a certain region. When QDs localized in regions with high oxygen density, such as lysosomes and mitochondria, the ratio of  $\text{O}_2$  to QD is high, which would result in a fast photobleaching. It has been reported that in lymphocytes the endosomes (lysosomes) were the binding sites of QDs [27]. Here, in HEK 293 cells, lysosomes are probably the QD localization sites too, which could be one of the reasons for the relatively fast photobleaching in HEK 293 cells.

To avoid fast photobleaching, increasing QD concentration is necessary, especially for those subcellular organelles with high oxygen density. However, the high concentration of cellular QDs may cause cytotoxicity in cells [28, 29]. The surface treatment or surface coating of the QDs with a shell can decrease the cytotoxicity in cells [30, 31], and also decrease the QD photo-oxidation due to the shielding effect of the shell [32, 33]. Thus, in the application of cellular labelling, the surface modification of QDs, such as coating the QD core or conjugation with biomolecules, should be considered.

#### 4. Conclusion

The rate of photobleaching of thiol-capped CdTe QDs inside living cells was dependent on the local concentration of cellular QDs and the irradiation intensity. Higher irradiation power density and oxygen density and lower QD concentration will result in a higher photobleaching rate. Such bleaching was found to be mainly due to the photo-oxidation of the cellular QDs. To avoid overly rapid photobleaching in experiments, such as cellular imaging, the local concentration of cellular QDs should reach a certain level and the over-irradiation must be avoided.

#### Acknowledgments

This work is supported by Shanghai Municipal Science and Technology Commission (03DJ14001 and 04DZ05617) and the National Natural Science Foundation of China (60578045).

## References

- [1] Stephens D J and Allan V J 2003 *Science* **300** 82
- [2] Weijer C J 2003 *Science* **300** 96
- [3] Bruchez M, Moronne M, Gin P, Weiss S and Alivisatos A P 1998 *Science* **281** 1013
- [4] Chan W C W and Nie S M 1998 *Science* **281** 2016
- [5] Chan W C W, Maxwell D J, Gao X H, Bailey R E, Han M Y and Nie S M 2002 *Curr. Opin. Biotechnol.* **13** 40
- [6] Parak W J, Gerion D, Pellegrino T, Zanchet D, Micheel C, Williams S C, Boudreau R, Le Gros M A, Larabell C A and Alivisatos A P 2003 *Nanotechnology* **14** R15
- [7] Alivisatos P 2004 *Nat. Biotechnol.* **22** 47
- [8] Qu L and Peng X 2002 *J. Am. Chem. Soc.* **124** 2049
- [9] Kippeny T, Swafford L A and Rosenthal S J 2002 *J. Chem. Educ.* **79** 1094
- [10] Yu W W, Qu L H, Guo W Z and Peng X G 2003 *Chem. Mater.* **15** 2854
- [11] Gao X H, Chen C W and Nie S M 2002 *J. Biomed. Opt.* **7** 532
- [12] Parak W J, Pellegrino T and Plank C 2005 *Nanotechnology* **16** R9
- [13] Kapitonov A M, Stupak A P, Gaponenko S V, Petrov E P, Rogach A L and Eychmuller A 1999 *J. Phys. Chem. B* **103** 10109
- [14] Gao X H and Nie S M 2003 *Trends Biotechnol.* **21** 371
- [15] Hanaki K, Momo A, Oku T, Komoto A, Maenosono S, Yamaguchi Y and Yamamoto K 2003 *Biochem. Biophys. Res. Commun.* **302** 496
- [16] Aldana J, Wang Y A and Peng X G 2001 *J. Am. Chem. Soc.* **123** 8844
- [17] Zhang H, Wang L, Xiong H, Hu L, Yang B and Li W 2003 *Adv. Mater.* **15** 1712
- [18] Guo J, Yang W and Wang C 2005 *J. Phys. Chem. B* **109** 17467
- [19] Kang L, Shen Z Q and Jin C Z 2000 *Chin. Sci. Bull.* **45** 585
- [20] Kim I S, Lee S K, Park Y M, Lee Y B, Shin S C, Lee K C and Oh I J 2005 *Int. J. Pharm.* **298** 255
- [21] Xu Y, Sun H C, Tian B, Li Y, Chen J, Chen J, Gao D M, Xue Q and Tang Z Y 2004 *J. Cancer Res. Clin. Oncol.* **130** 375
- [22] Brown J S 1980 *Biochim. Biophys. Acta* **591** 9
- [23] Einicker-Lamas M, Mezian G A, Fernandes T B, Silva F L S, Guerra F, Miranda K, Attias M and Oliveira M M 2002 *Environ. Pollut.* **120** 779
- [24] Li Z F and Ruckenstein E 2004 *Nano Lett.* **4** 1463
- [25] Hoshino A, Hanaki K, Suzuki K and Yamamoto K 2004 *Biochem. Biophys. Res. Commun.* **314** 46
- [26] Smith A M, Gao X and Nie S 2004 *Photochem. Photobiol.* **80** 377
- [27] Hoshino A, Nanaki K I, Suzuki K and Yamamoto K 2004 *Biochem. Biophys. Res. Commun.* **314** 46
- [28] Derfus A M, Chan W C W and Bhatia S N 2004 *Nano Lett.* **4** 11
- [29] Kloepper J A, Bradforth S E and Nadeau J L 2005 *J. Phys. Chem. B* **109** 9996
- [30] Hoshino A, Fujioka K, Oku T, Suga M, Sasaki Y F, Ohta T, Yasuhara M, Suzuki K and Yamamoto K 2004 *Nano Lett.* **4** 2163
- [31] Kirchner C, Liedl T, Kudera S, Pellegrino T, Javier A M, Gaub H E, Stolzle S, Fertig N and Parak W J 2005 *Nano Lett.* **5** 331
- [32] Spanhel L, Haasse M, Weller H and Henglein A 1987 *J. Am. Chem. Soc.* **109** 5649
- [33] Nirmal M, Dabbousi B O, Bawendi M G, Macklin J J, Trautman J K, Harris T D and Brus L E 1996 *Nature* **383** 802